Peptide-guided self-assembly of polyethylene glycol-b-poly(ε-caprolactone-g-peptide) block copolymers

Ayman El Jundi, Matthias Mayor, Enrique Folgado, Chaimaa Gomri, Belkacem Tarek Benkhaled, Arnaud Chaix, Pascal Verdie, Benjamin Nottelet, M. Semsarilar

Peptide-guided self-assembly of polyethylene glycol-*b*-poly(ε-caprolactone-*g*-peptide) block copolymers

Ayman El Jundi[1‡], Matthias Mayor[2‡], Enrique Folgado[2], Chaimaa Gomri[2], Belkacem Tarek Benkhaled[2], Arnaud Chaix[2], Pascal Verdie[3], Benjamin Nottelet[1*], Mona Semsarilar[2*]

[1] Department of Polymers for Health and Biomaterials, IBMM (UMR5247), Univ Montpellier, CNRS, ENSCM, Montpellier, France

[2] Institut Européen des Membranes, IEM (UMR5635), Univ Montpellier, CNRS, ENSCM, Montpellier, France

[3] Synbio3, IBMM (UMR5247), Univ Montpellier, CNRS, ENSCM, Montpellier, France

corresponding authors : benjamin.nottelet@umontpellier.fr, mona.semsarilar@umontpellier.fr

Abstract

Biodegradable poly(ethylene glycol)-*b*-poly(ε-caprolactone-*g*-peptide) (PEG-*b*-PCL-*g*-peptide) copolymers were synthesized using a combination of ring opening polymerization and thiol-yne photoaddition of peptides on the alkyne functional PCL block. The peptides Phe-Phe, Tyr-Tyr and Arg-Gly-Asp were selected based on the expected interactions (Pi-stacking, H-bonding, electrostatic). The self-assembly of these copolymers was studied via testing the effect of various parameters such as the nature of the solvent and non-solvent as well as their ratio, mixing method, temperature and concentration. Structures obtained by varying these parameters were characterised using transmission electron microscopy (TEM) and dynamic light scattering (DLS). Spherical and lamellar structures (oval leaf-shaped) of different sizes were identified as a function of the conditions. The role of the crystallisation and of the peptides was highlighted with more defined and stable structures obtained for Tyr-Tyr functional copolymers.

Key words: Solution self-assembly, ring opening polymerization, click reaction, thiol-yne, block copolymers, peptide, poly(caprolactone), poly(ethylene glycol), temperature induced crystallization induced self-assembly (TI-CDSA).

Introduction

The control of the structures of polymers in solution is of prime importance in biomedical applications as this structuring defines the activity of the resulting self-assemblies. This is in particular true when peptides are used to guide this structuring as they can confer biofunctionality (*eg.* collagen like peptides[1]), or bioactivity (*eg.* IKVAV for fibroblasts and neurone proliferation[2]) to the self-assemblies. Not surprisingly, PEG has been largely used in peptide—polymer conjugates to evaluate the influence of the selected peptides on the peptide-guided structures and formation of supramolecular self-assemblies ranging from micelles, to ribbons, membranes or even fibres.[3] On the other hand, PEG has also largely been used as hydrophilic block in amphiphilic block copolymers that are widely exploited for drug encapsulation and delivery. Among them, PEG-polyester block copolymers having a hydrophobic polylactide (PLA), polyglycolide (PGA, or poly(ε-caprolactone) (PCL) block are the most studied examples due to their long track record and regulatory acceptance.[4] However, the combination of peptide-guided structuring and PEG-polyester block copolymers is rarely described and most examples relate to the copolymer chain-end functionalization with a targeting peptide moiety able to enhance the accumulation of the resulting self-assemblies into specific tissues. One of the best examples is the peptide Arg-Gly-Asp under its linear (RGD) or cyclic (cRGD) form that is able to target the integrins present at the surface of cells and overexpressed in most cancer cells and is therefore present in countless drug delivery systems.[5, 6] The absence of PEG-polyester peptide guided self-assemblies is in particular true for PCL-based systems. PCL being less degradable and more hydrophobic than PLA and PGA, it is less used to develop novel self-assemblies for biomedical applications. However, these characteristics explain that PEG-PCL copolymers yield highly stable micelles and nanoaggregates, which make them particularly interesting to develop long lasting drug delivery systems. In this frame, PEG-*b*-PCL copolymers have been end-functionalized with various peptides including RGD for targeted bioimaging,[7-9] cell penetrating peptide or glioma-homing peptides for enhanced gliomas treatment,[10, 11] tumor metastasis targeting for delivery to metastatic cells.[12] Replacing peptides chain end by polypeptides was also recently illustrated with the design of PEG-*b*-PCL-*b*-polytyrosine triblock copolymers allowing enhanced drug/polymer interactions, higher drug loading and micelles stability.[13] Alternatively to the modification at the PEG-*b*-PCL chain ends, central peptide block is also conveniently reported to yield enzyme-cleavable block copolymers with a sheddable PEG shell.[14] Multi-functionalization with targeting and/or enzyme-cleavable peptides has also

been reported in more complex macromolecular topologies including comb and graft PCL-based copolymers to benefit from higher content of peptides and therefore obtain higher biological outputs.[15-17]

In agreement with the final application as injectable drug delivery systems, all these copolymers were designed to self-assemble into spherical nano-micelles or nano-aggregates. More rarely, such amphiphilic PEG-PCL peptide conjugates have been directly used to generate bioactive materials, like for example RGD-functionalized nanofibers by electrospinning.[18]

These examples clearly illustrate the interest in these PEG-PCL peptide conjugates to induce bioactivity. However, there are only few examples of studies dedicated to the impact of the peptides to physically control the association/dissociation and the morphology of the PEG-PCL self-assemblies. Katz *et al.* inserted a peptide between the PEG block and the PCL block using an approach inspired by solid-phase peptide synthesis. They prepared photolabile PEG-*b*-PCL copolymers containing a 2-nitrophenylalanine central unit to generate polymersomes that can undergo UV-induced cleavage.[19] In another example, Ding *et al.* prepared poly(ε-caprolactone-*co*-lactide) (PCLA) triblock copolymers (PCLA–PEG–PCLA) able to form hydrogels via bridging of flower-micelles. This triblock was functionalized with cRGD moieties (ca. 10 mol% with respect to polymer chains) located either at both chain-ends via classical amidation, or randomly dispersed along the PEG block thanks to the photo-insertion of 4-(*p*-azidophenyl)-*N*-succinimidyl butanoate and subsequent addition of cRGD. Although the impact on self-assembly was not discussed, it was found that the chain conformations and therefore the spatial presentation of the cRGD had an impact on chondrocytes adhesion.[20]

In this work, we prepared functional PEG-*b*-PCL copolymers with peptides grafted along the PCL block to investigate the impact of the selected peptides on the self-assembly behavior of the PEG-PCL peptide conjugates. The rational for selecting a functionalization along the PCL backbone and not on the PEG chain-end or between the blocks as reported in the literature is to take advantage of the multi-functionalization of the PCL backbone to enhance the potential impact of the peptides on the self-assembly. Three peptides containing the Phe-Phe motif for Pi-stacking interactions, Tyr-Tyr for Pi-stacking and H-bonding interactions, and Arg-Gly-Asp for H-bonding and electrostatic interactions, have been selected. These three peptides were selected based on their simple structure allowing comparison as a function of the interactions and an easier production, and for the last one its potential bioactivity.

EXPERIMENTAL SECTION

Materials

α-methoxy,ω-hydroxyl poly(ethylene glycol) (PEG$_{2k}$ Mn=2000 g/mol), stannous octoate (Sn(Oct)$_2$, 92.5-100%), ε-caprolactone (CL, 97%), 2.2-dimethoxy-2-phenyl-acetophenone (DMPA, 99%), propargyl bromide (PgBr, 80 wt% in toluene), lithium diisopropylamide (LDA, 2 M in THF/heptane/ethylbenzene) were purchased from Sigma-Aldrich (St-Quentin Fallavier, France). THF was dried using a Pure Solv Micro Single Unit (Inert®) system. Toluene was distilled over CaH$_2$, and DMSO was dried over molecular sieves (4Å) prior to use. PEG was dried by an azeotropic distillation in dry toluene. ε-CL was dried over calcium hydride (CaH$_2$) for 48 h at room temperature and distilled under reduced pressure. Ac-Cys-Gly-Tyr-Tyr-CONH$_2$ (peptide 1), Ac-Cys-Gly-Phe-Phe-CONH$_2$ (peptide 2) and Ac-Cys-Gly-Arg-Gly-Asp-OH (peptide 3) were provided by the platform Synbio3 (https://ibmm.umontpellier.fr/synbio3/).

Characterizations and methods.

Nuclear magnetic resonance spectroscopy (NMR). ^{1}H NMR (300 MHz) spectra were recorded on a Bruker AMX300 spectrometer at 25 °C. Deuterated chloroform and deuterated dimethyl sulfoxide were used as solvent, chemical shifts were expressed in ppm with respect to tetramethylsilane (TMS).

Size exclusion chromatography (SEC). The number-average and weight-average molar masses (Mn and Mw, respectively) and dispersity (Đ, Mw/Mn) of the polymers were determined by SEC using a Viscotek GPCmax VE2100 liquid chromatograph equipped with a Viscotek VE3580 refractive index detector operating at 35 °C. Tetrahydrofuran was used as the eluent and the flow rate was set up at 1.0 ml/min. Two LT5000L 300 x 7.8 mm columns operating at 29°C were used. Calibrations were performed with polystyrene standards. For analyses in DMF, a Waters Inc. equipment fitted with a 5 μm mixed C PLgel 5 μm MIXED-D (300×7.5 mm) operating at 60°C and SHODEX RI 101 refractometric detector was used. The mobile phase was DMF at 0.8 mL/min flow. Typically, the polymer (10 mg) was dissolved in DMF (2 mL) and the resulting solution was filtered through a 0.45 μm Millipore filter before injection of 20 μL of a filtered solution. Calibrations were performed with poly(methyl methacrylate) standards.

Differential scanning calorimetry (DSC). The thermograms were obtained from a TA instrument Q20 DSC. The dry samples were placed in a sealed pan. The analyses were performed from -100°C to 150°C with a temperature gradient of 10°C/min. The results were analysed using TA Universal Analysis software.

Transmission electronic microscopy (TEM). TEM studies were conducted using a JEOL 1400+ instrument equipped with a numerical camera, operating with a 120 kV acceleration voltage at 25 °C. To prepare TEM samples, a drop (10.0 μL) of micellar solution was placed onto a Formvar/Carbon coated copper grid for 60 s, blotted with filter paper and dried under ambient conditions. All TEM grids were prepared from self-assembly experiment solutions without further dilution.

Dynamic light scattering (DLS). DLS measurements were conducted on an Anton-Paar Litesizer 500 using a quartz cuvette without further dilution.

Synthesis and characterization of PEG-*b*-PCL-*g*-peptides

Synthesis of copolymer PEG-b-PCL (C1).

The amphiphilic PEG-*b*-PCL diblock copolymers were synthesized by ring opening polymerization (ROP) of ε-caprolactone in toluene at 100°C. α-methoxy,ω-hydroxyl poly(ethylene glycol) and stannous octoate were used as initiator and catalyst, respectively. In a typical procedure, to a solution of PEG_{2K} (3g; 1.5 mmol) in 25 mL of toluene in a Schlenk tube, CL (3g; 26 mmol) and $Sn(Oct)_2$ (0.23 mL, 0.7 mmol) were added. Following freeze-pump-thaw cycles, the reaction was allowed to proceed for 24 h at 100 °C in a nitrogen atmosphere. The product was precipitated in a large excess of cold diethyl ether. PEG-*b*-PCL was obtained by filtration and dried 24 h in vacuo at room temperature (copolymer **C1**, Scheme 1). Yield 87%

^{1}H NMR (300 MHz, CDCl$_3$): δ =4.05 (t, CH$_2$C*H$_2$*OCO), 3.64 (m, OC*H$_2$*CH$_2$O), 3.34 (s, C*H$_3$*O), 2.30 (t, COC*H$_2$*CH$_2$), 1.65 (m, COCH$_2$C*H$_2$*CH$_2$C*H$_2$*CH$_2$O), 1.39 (m, COCH$_2$CH$_2$C*H$_2$*CH$_2$CH$_2$O). SEC (THF): M$_n$ = 4500 g/mol, Đ = 1.1.

Propargylation of copolymer PEG-b-PCL (C2).

Propagylation of PEG-*b*-PCL was performed according to a procedure reported by our group.[21] Typically, PEG$_{1900}$-*b*-PCL$_{1700}$ (1g, 4.1 mmol of CL) was suspended in 25 ml of anhydrous toluene under inert gas in a 3-neck flask. After cooling to -50°C, a solution of LDA

(2.1 mmol, 0.5 eq. per CL unit) in a mixture of THF/heptane/ethylbenzene was added under agitation via injection through a septum. After stirring for 15 min at -50 °C, a solution of PgBr (8.2 mmol, 2 eq. per CL unit) in toluene was added. The reaction was quenched after 15 min by addition of 1 M HCl solution until neutral pH. The crude reaction mixture was transferred to a dialysis bag (MWCO 3500 g/mol, Spectra-Por) and dialyzed against a mixture of water and acetone (1/1, v/v) for 1 d. After evaporation of acetone under reduced pressure, PEG-*b*-PCL(YNE) was obtained by lyophilization (copolymer **C2**, Scheme 1). Yield 85%.

^{1}H NMR (300 MHz, CDCl$_3$): δ = 4.1 (t, CH$_2$C*H$_2$*OCO), 3.65 (m, OC*H$_2$*C*H$_2$*O), 3.33 (s, C*H$_3$*O), 2.6-2.4 (m, COC*H*CH$_2$CCH and C*H$_2$*CCH), 2.30 (t, COC*H$_2$*CH$_2$), 2.0 (s, CH$_2$CC*H*), 1.85 (m, COCHC*H$_2$*CH$_2$C*H$_2$*CH$_2$O), 1.65 (m, COCH$_2$C*H$_2$*CH$_2$C*H$_2$*CH$_2$O), 1.38 (m, COCH$_2$CH$_2$C*H$_2$*CH$_2$CH$_2$O). SEC (THF): M$_n$ = 4200 g/mol, Đ = 1.3. Substitution degree with respect to CL units 15% (from NMR analysis).

Grafting of peptides on PEG-b-PCL(YNE) (CP1-CP3)

Grafting of peptides on the multi-alkyne functional copolymer was achieved by adapting protocols of our group.[17] Typically, PEG-*b*-PCL(YNE) (150 mg, 15% alkyne groups with respect to CL units) and peptide 1 (Ac-Cys-Gly-Tyr-Tyr-NH$_2$ 341 mg; 8 eq. with respect to initial alkyne group) were dissolved in 4 mL DMF in a Schlenk flask. In parallel, DMPA (81 mg; 4 eq. with respect to initial alkyne group) was dissolved in 0.5 mL DMF and the solution was protected from light using aluminium foil. The solution of the DMPA was then added to the polymer/peptide solution, the flask was closed by septum and purged with argon for 10 min under nitrogen in the dark. The reaction mixture was then irradiated with UV light. Reaction was carried out for 2 hours under constant stirring and constant UV light irradiation (Dymax Blue wave® 200, 100 mW/cm2). For purification, the reaction mixture was initially diluted with water to reach a 50:50 water/DMF ratio prior to dialysis against water using a centrifugal filter unit (MW cut-off 10 000 Da) (10 cycles of centrifugations). The copolymer was freeze-dried (copolymer **CP1**, Scheme 1). Yield 40%. For peptides 2 and 3, the conditions of reaction are listed in Table S2 (copolymer **CP2 and CP3**, Scheme 1).

^{1}H NMR CP1 (300 MHz, DMSO-d6): δ =8.5-7.5 (m, N*H*CO), 7.5-7.0 (m, C*H* ar and N*H$_2$*), 4.50-4.25 (m, NHC*H*CO and -O*H*), 4.05 (t, CH$_2$C*H$_2$*OCO), 3.75 (m, NHC*H$_2$*CO), 3.64 (m, OC*H$_2$*C*H$_2$*O), 3.20-2.60 (m, CHC*H$_2$*), 2.30 (t, COC*H$_2$*CH$_2$), 1.85 ppm (s, C*H$_3$*CO) 1.65 (m, COCH$_2$C*H$_2$*CH$_2$C*H$_2$*CH$_2$O), 1.39 (m, COCH$_2$CH$_2$C*H$_2$*CH$_2$CH$_2$O). SEC (DMF): M$_n$ = 2800 g/mol, Đ = 2.4.

Self-assembly of peptide-functionalized copolymers

Preparation of stock solutions

Stock solutions of 0.5 and 1 mg.mL^{-1} were prepared in DMF and DMSO, at room temperature. To ensure full solubilization, solutions were left stirring for 3h.

Nanoprecipitation

Glass vials containing 1 mL of non-solvent or selective solvent for the PEG (i.e. water or ethanol) were placed on a stirring plate. To each vial, 0.1 mL of stock solution was added dropwise and left stirring for 1h. The solutions obtained were analysed by DLS and TEM.

Micellization

Vials containing 0.5 mL of stock solutions were placed in a shaker. Water was added slowly using a syringe pump at a fixed rate (0.04mL.min^{-1} or 2.4 mL.min^{-1}). Samples were prepared at 1: 4; 1: 6 and 1: 8 solvent/ non-solvent ratios.
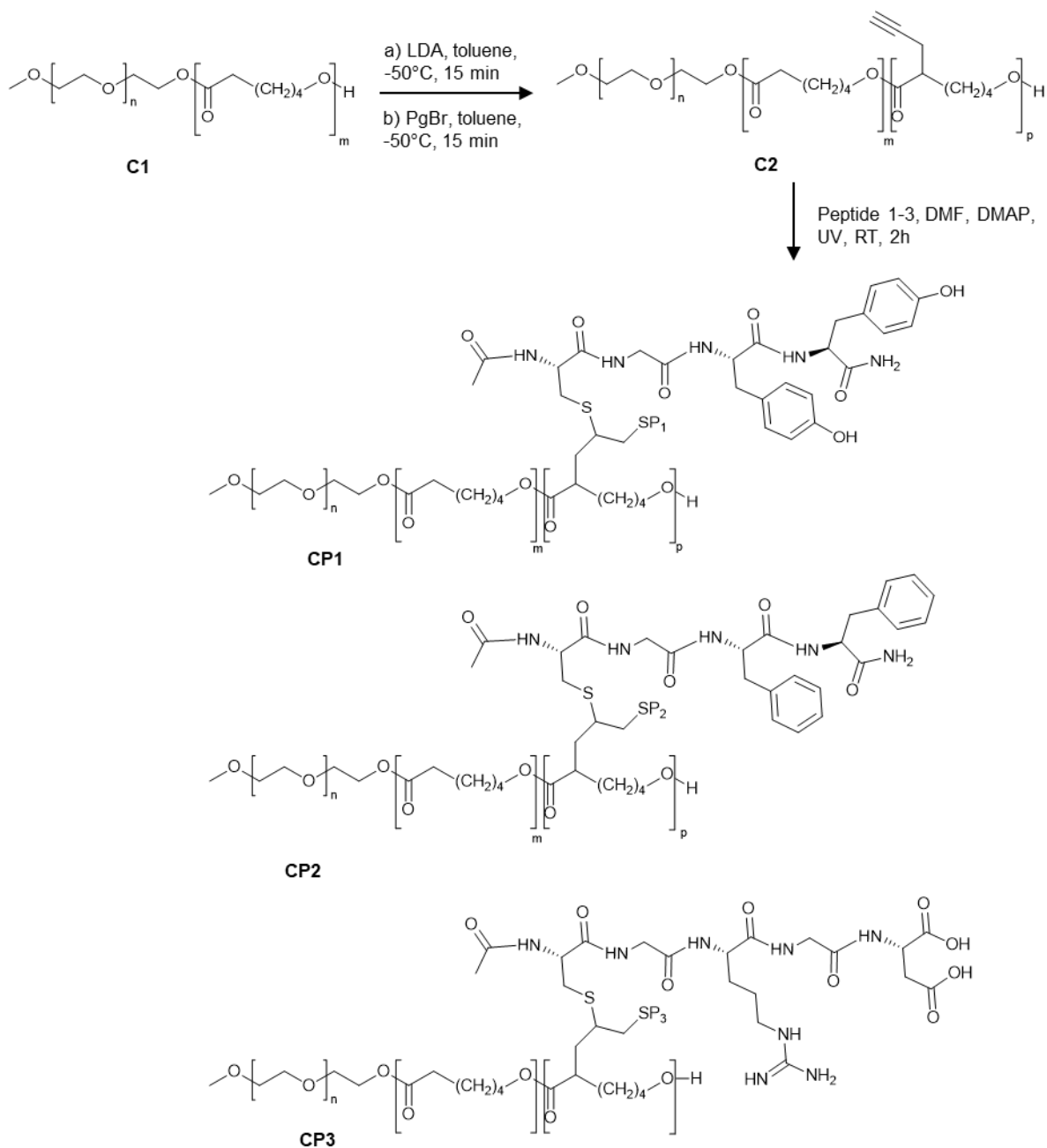
Scheme 1. Synthesis pathway for the preparation of peptide-functionalized copolymers CP1, CP2 and CP3.

RESULTS AND DISCUSSION

1. Synthesis of copolymers

The copolymers functionalized with peptides were prepared in three steps. First, an amphiphilic PEG$_{2k}$-*b*-PCL$_{2k}$ block copolymer was prepared by ring opening polymerization of CL using PEG$_{2k}$ as a macroinitiator (C1, Scheme 1). A molecular weight of 2000 g/mol for the PCL block was targeted and confirmed both by ^{1}H NMR using the ratio between the integrals of peaks at 3.64 ppm and at 4.05 ppm corresponding to the methylene protons of EG and CL units, respectively (Figure S1). It was also confirmed by SEC with Mn = 4500 g/mol and a low dispersity of 1.1. In a second step, the PCL block was functionalized with alkyne groups by anionic modification of the CL units according to a well-established procedure (C2, Scheme 1).[21] Using LDA and PgBr, 15% of the CL units were functionalized with a pendant propargyl group. This substitution degree was calculated from the ^{1}H NMR spectra (Figure S2) by comparing the integral of the signal at 2.4-2.6 ppm with the integral of the PCL methylene signal at 4.1 ppm. The ^{1}H NMR spectrum also showed a limited molecular weight decrease of the PCL block from 2000 g/mol to 1600 g/mol (1% hydrolyzed ester bonds) that was also confirmed by SEC with Mn = 4200 g/mol and a dispersity of 1.3. The final step corresponded to the functionalization of the resulting PEG-*b*-PCL(YNE) with the selected peptides (Table S1). The grafting of peptides on the backbone of C2 was achieved by thiol-yne photoaddition between the thiol groups of the cysteine moieties present in the peptides and the alkyne groups of C2. Conditions were adapted from our previous work and are summarized in Table S2.[17, 21] The substitution degree was estimated using the ^{1}H NMR spectra by comparing the integrals of the methylene groups of PCL and the methyl group of the acetamide group at 1.85 ppm present on all peptides and results are listed in Table S2. The photoaddition efficiency was function of the nature of the peptide with 50% of peptide 1 photoaddition for CP1 (Cys-Gly-Tyr-Tyr-NH$_2$ peptide) and 25% for CP3 (Cys-Gly-Arg-Gly-Asp-OH peptide). Grafting and purity were confirmed by DOSY-NMR and SEC as exemplified with CP1 (Figure S6 and S8). In particular, DOSY-NMR analysis of CP1 showed peaks characteristics of peptide 1 and of C2 at the same coefficient of diffusion (Figure S8). It should be noted that it was not possible to calculate the extent of functionalization for CP2 due to the presence of free residual peptide 2 that was detected as a second peak on the SEC chromatogram despite the purification steps (Figure S6). For CP3 the SEC chromatograms showed three populations with a first low intensity peak corresponding to low amounts of residual free peptide 3, a peak of highest intensity corresponding to the copolymer CP3 and a last peak towards higher molecular weights

that was attributed to CP3 aggregates (Figure S6). The grafting of peptide 3 was further confirmed by DOSY-NMR with signals characteristic of peptide 3 and of C2 at the same coefficient of diffusion ((Figure S9). Of notice, free Peptide 3 was not visible on this analysis confirming the low content of non-grafted peptide in CP3. "It should be noted that, the broadening of the distribution and apparent decrease of the molecular weight after peptide-functionalization was noticed. For example, for CP1 Mn of 2800 g/mol and a dispersity of 2.4 were measured. However, this result should be considered with care as the hydrodynamic behavior of the copolymers is known to be strongly affected by their amphiphilicity and architecture. This is why the presented copolymers with changes of chain conformations due to both a shift from a linear PEG-b-PCL(YNE) to a polymer with bulky grafted peptides and a change of amphiphilicity that depends on the peptides nature."

2. Self-assembly

The synthesized peptide functionalized copolymers were self-assembled via two pathways: micellization (gradual addition of non-solvent to the polymer solution) or nanoprecipitation (addition of polymer solution to non-solvent). Due to the difficulties encountered to purify CP2 that contained high amount of free peptide 2 despite purification steps, this copolymer was not further investigated in this part. Both CP1 and CP3 were soluble in DMF and DMSO. CP1 and CP3 were designed to be amphiphilic thanks to the PCL hydrophobic block and the PEG hydrophilic block. The difference resides in the nature of the pending peptides on the PCL segment. Having two tyrosine per substituent, CP1 is expected to present Pi-stacking and H-bonding interactions.[22] In contrast, the CP3 with arginine and aspartic acid amino acids is expected to exhibit only H-bonds.

2.1. CP1 Micellization

DMF was used as the common solvent for the blocks and water as a non-solvent (selective solvent for PEG). Different ratios of solvent/ non-solvent were used. A mother solution with concentration of 1 mg / mL in DMF was used and 1: 4; 1: 6 and 1: 8 ratios of solvent/ non-solvent were prepared. For the ratio 1: 4, particles of 20 nm and 1µm were detected by DLS. For the other two ratios, particles of 30 nm and 1.5µm were measured. TEM images of these samples showed mainly aggregates (Figure 1). Spherical particles and nanoaggregates of different size were detected for the three ratios tested. Some flat structures were also observed for 1: 6 and 1: 8 ratios (Figure 1D-E). One reason for the ill-defined structures observed could

be the poor solubility of the PCL block in DMF.[23] The same behaviours was observed for the PEG-*b*-PCL (**C2**) with no grafted peptide used as the control reference (Figure S10).
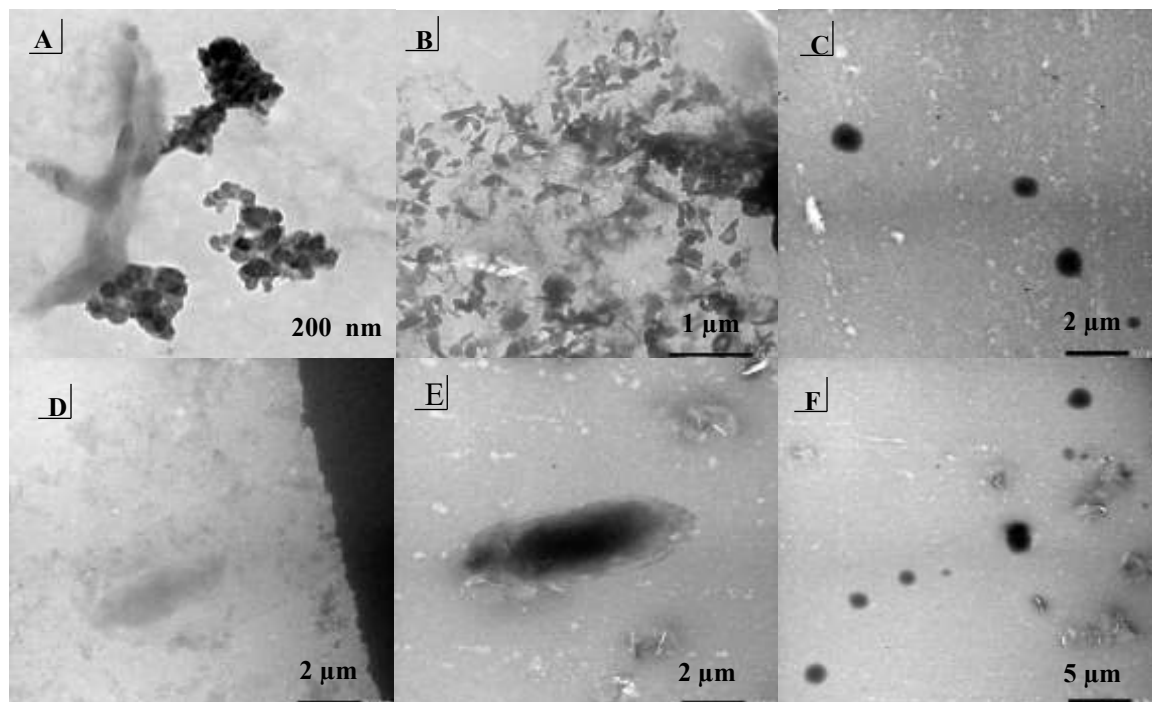

Figure 1: TEM images of self-assembled CP1 via micellization in DMF/H$_2$O at ratios of (A-B) 1:4 (C- D) 1:6 (E-F) 1:8.
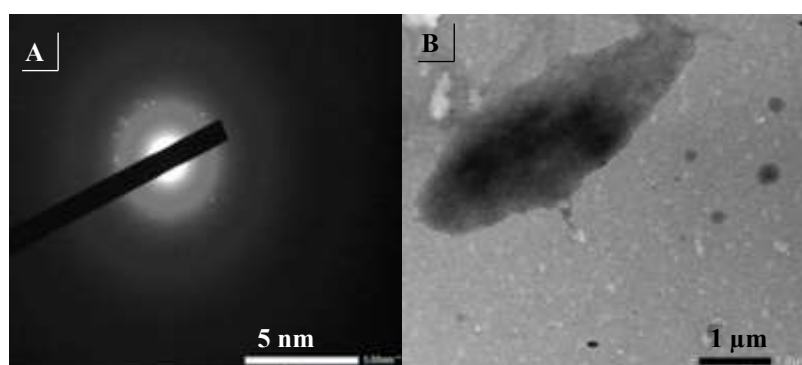

Figure 2. Diffraction pattern and TEM image of CP 1 with lamella flat structure.

Figure 2, shows the diffraction pattern of the flat lamella structure observed for the DMF/H$_2$O 1:8 ratio. The scintillating dots (Figure 2A) suggests certain degree of crystallinity. This is certainly due to the crystalline PCL (Figure S13). It was observed that the structure became

amorphous after being exposed to the electron beam. This is due to the thin self-assembled structure.

In order to increase the solubility of the PCL block, instead of DMF, DMSO was used.[23] The self-assembly in 1:4 ratio of DMSO/ H_2O resulted in the formation of two populations; nano-objects around 30 nm along with larger objects with average size of 2µm as measured by DLS. These size where in agreement with the size observed in TEM images. As shown in Figure 3, well defined large lamellar micelles along with small spheres could be seen. Increasing the water content did not change the morphology. This is most probably due to the combination of the crystallinity of the PCL at room temperature and of the potential strong interactions between the tyrosine groups (Pi-stacking and H-bonding) that both could inhibit the evolution of the morphology. In addition, the high substitution degree of substitution of CP1 the tyrosine-functionalized PCL block could lead to behaviors close to the ones of PEG-*b*-Poly(tyrosine) recently reported that lead to supramolecular assemblies such as micelles, fibrils or even β-amyloid structures as a function of the hydrophilic/hydrophobic balance.[24] It should be noted that using the same conditions with C2 did not result in formation of such lamellar micelles, confirming the role of the Tyr-Tyr moieties in driving the self-assembly of **CP1** (Figure S11).
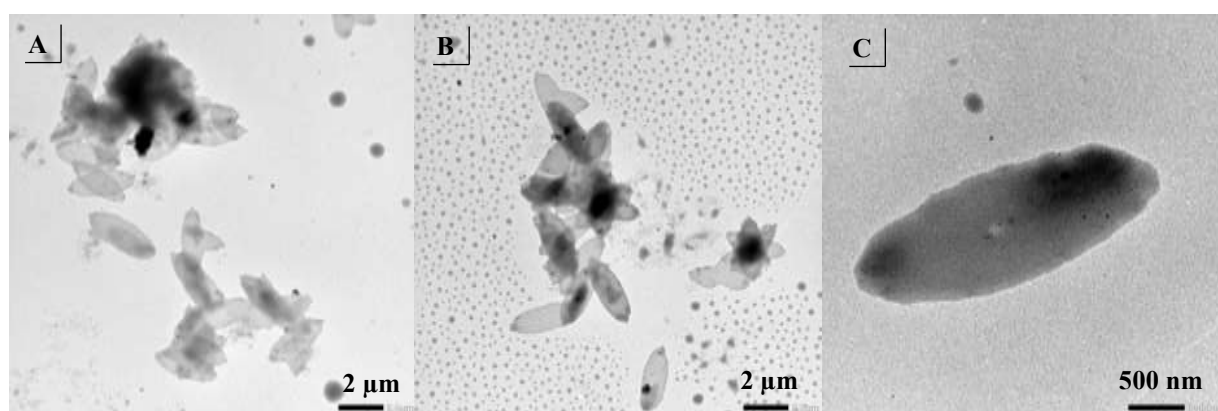

Figure 3. TEM images of self-assembled CP1 via micellization in DMSO/H_2O at ratio of 1:4.

Next, micellization of PC1 in DMF/ H_2O was carried out in a sonication bath at 60 °C, under temperature-induced crystallization-driven self-assembly (TI-CDSA).[25] Performing the self-assembly at 60 °C mean that the PCL block would be at molten state. As observed under TEM, this time crystalline individual needles of 250 nm along with bundles of them resembling sea urchins were formed (Figure 4). These needles are definitely the result of self-assembling chains while PCL was at molten state and the gradual cooling and crystallization.
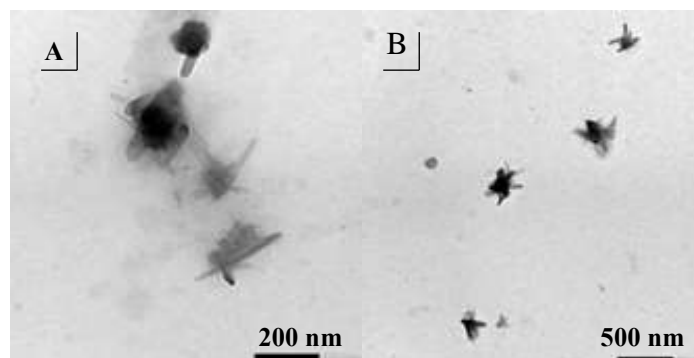
Figure 4. TEM images of self-assembled CP1 via TI-CDSA in DMF/H₂O at ratio of 1:4.

2.2. CP1 Nanoprecipitation

Nanoprecipitation was performed first with DMF/ H$_2$O. As shown in Figure 5, similar flat lamella objects were formed as in the case of micellization (Figure 1 and 3).   The DLS results were very different from the results observed in TEM. This difference is mainly due to the shape of the nano-objects that are far from the spherical morphology model inbuilt in the DLS software. Repeating this self-assembly path using a sonication bath at 60°C, well-defined multi-lamellar micelles of different size (2- 3µm) were formed. The dark centres and lighter edges suggest that several different layers of different size, flat lamellar micelles have over lapped upon drying (Figure 6). As in the case of micellization, such structures were not observed for **C2** (Figure S12).
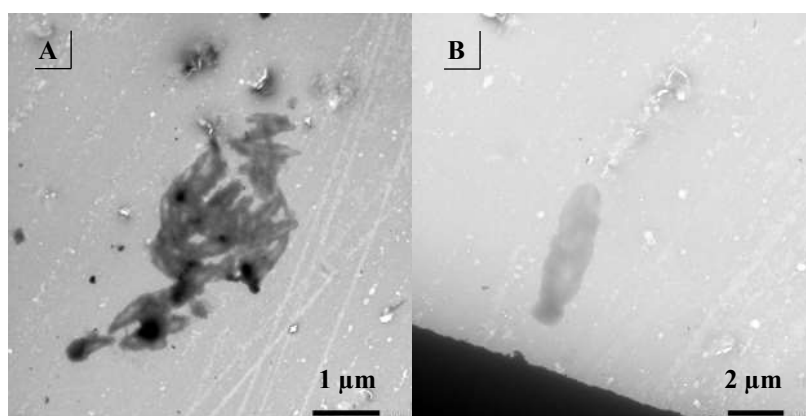

Figure 5. TEM images of self-assembled CP1 via nanoprecipitation in DMF/H$_2$O at ratio of 1:4.
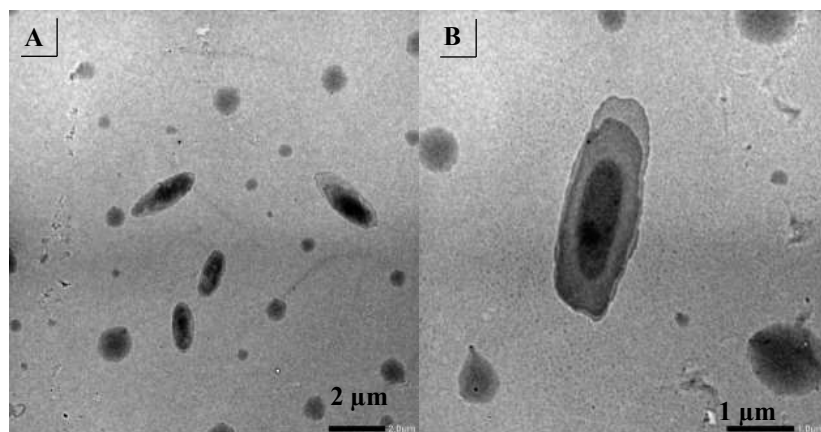
Figure 6. TEM images of self-assembled CP1 via TI-CDSA in DMF/H$_2$O at ratio of 1:4.

Changing the non-solvent (selective solvent for PEG) to ethanol did not result in formation of well-defined objects either as mainly aggregates were observed (Figure 7). Changing the solvent mixture to DMSO/ water or ethanol, only resulted in the formation of not very defined aggregates (Figure 8). As presented above CP1 mainly formed lamellar structures in the solvent/ non-solvent pairs tested. Although, using the TI-CDSA at 60 °C resulted in formation of more defined lamellar structures.
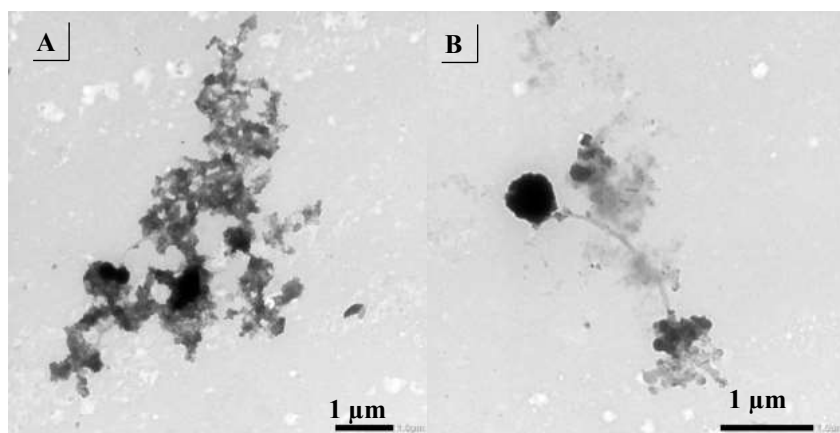

Figure 7. TEM images of self-assembled CP1 via nanoprecipitation in DMF/ethanol at ratio of 1:4.
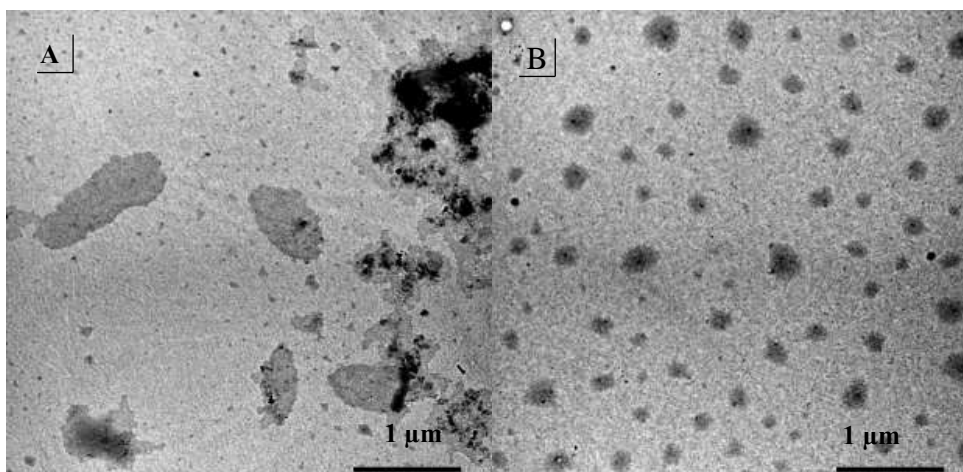
Figure 8. TEM images of self-assembled CP1 via nanoprecipitation in (A) DMSO/H₂O, (B) DMSO/ethanol at ratio of 1:4.

2.3. CP3 Micellization

As in the case of **CP1** same solvent/ non-solvent system along with self-assembly pathways were used. The self-assembly using DMF/ H_2O at different ratios of 1: 4; 1: 6 and 1: 8 from a 1 mg/mL polymer solution resulted in formation of aggregates of 2 µm no matter which solvent/ non-solvent ratio was used as judged by DLS. Even lowering the concentration of the polymer solution to 0.5 mg/mL did not change the size of the aggregates. TEM images (Figure 9) also confirmed the formation of large flat aggregates. Keeping the **CP3** stock solution concentration constant while changing the solvent/ non-solvent ratio (Figure 9 A, C, D) as well as changing the polymer concentration while keeping the same solvent/ non-solvent ratio (Figure 9 A-B) did not change the size or the morphology of the structures. Electron diffraction on micelles presented in Figure 9A, showed scintillating dots (Figure 10) suggesting some degree of crystallinity.
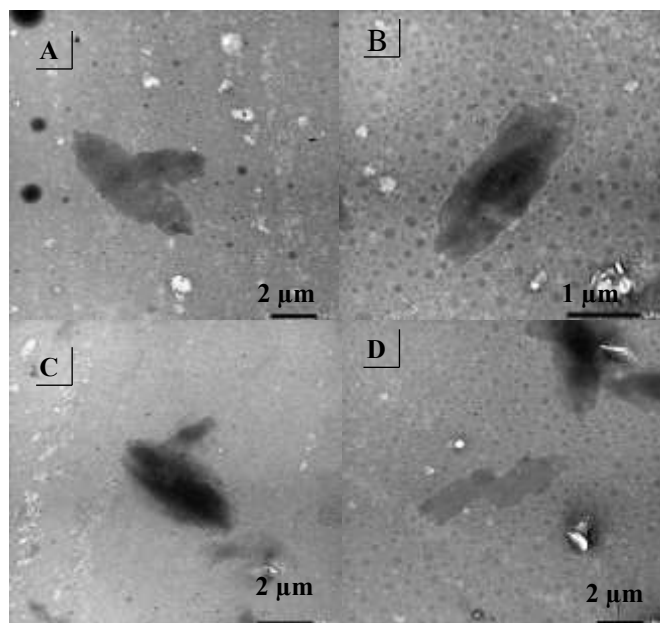
Figure 9. TEM images of self-assembled CP3 via micellization in DMF/H₂O from (A) 1mg/mL in 1:4 (B) 0.5 mg/mL in 1:4 (C) 1mg/mL in 1:6 (D) 1mg/mL in 1:8.
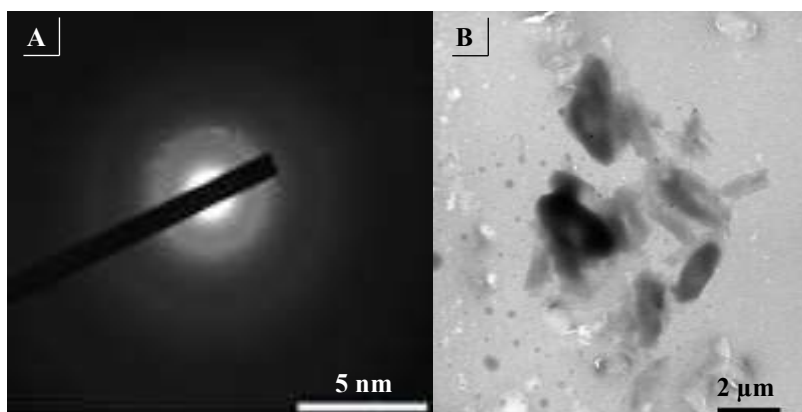

Figure 10. Diffraction pattern and TEM image of CP3 with lamella structure.

The self-assembly in water from CP3 dissolved in DMSO resulted in formation of structures of 100 nm and 2µm measured by DLS. TEM images also showed two populations of self-assembled structures. Dispersed spherical nanoparticles (35-95 nm) and large (~4.5 µm) flat lamellar structures (Figure 11).
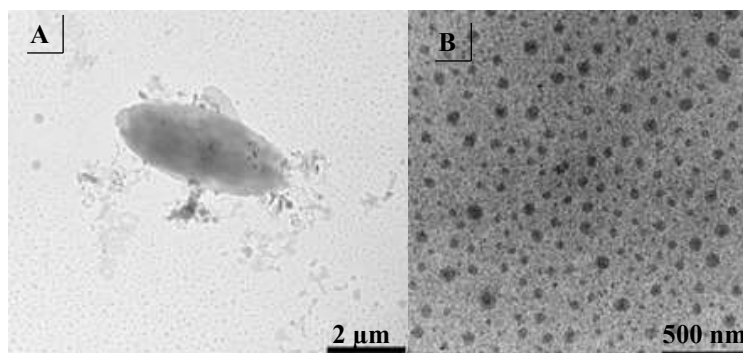
Figure 11. TEM images of self-assembled CP3 via micellization in DMSO/H₂O at 1:4.

2.4. CP3 Nanoprecipitation

Nanoprecipitation was performed in water or ethanol from a solution of CP3 dissolved in DMF (1 mg/mL). When nanoprecipitation was carried out using magnetic stirring, flat ribbons were formed. They looked disconnected, as if flat narrow layers of self-assembled micelles were overlapping to form long fibres (Figure 12 A-B). Next, the self-assembly was carried out in an ultra-sonication bath at 60 °C. As shown in Figure 12 C-D, large flat structures with dark centres were observed. Formation of such structures are more likely due to the fact that the self-assembly took place above the melting point of the crystalline PCL. Being at molten state, along with gradual cooling allows the slow re-crystallization of the PCL chains, giving time to the entire system to self-assemble into a more defined morphology. Changing the non-solvent to ethanol (with magnetic stirring) did not allow formation of well-defined structures as many aggregates could be seen on the TEM grid (Figure 12 E-F). The DLS analysis of these samples were not conclusive as the structures are very irregular.

Finally, the self-assembly via nanoprecipitation was repeated using DMSO as the good solvent. When both water and ethanol were used as the non-solvent, instead of fibrous structures (as in the case of DMF/ water) only ill-defined spheres and some bilayers were formed (Figure 13). These results suggest that DMSO is not as good solvent for CP3 as compared to CP1, since well-defined objects were formed with CP1 using DMSO as the solvent.
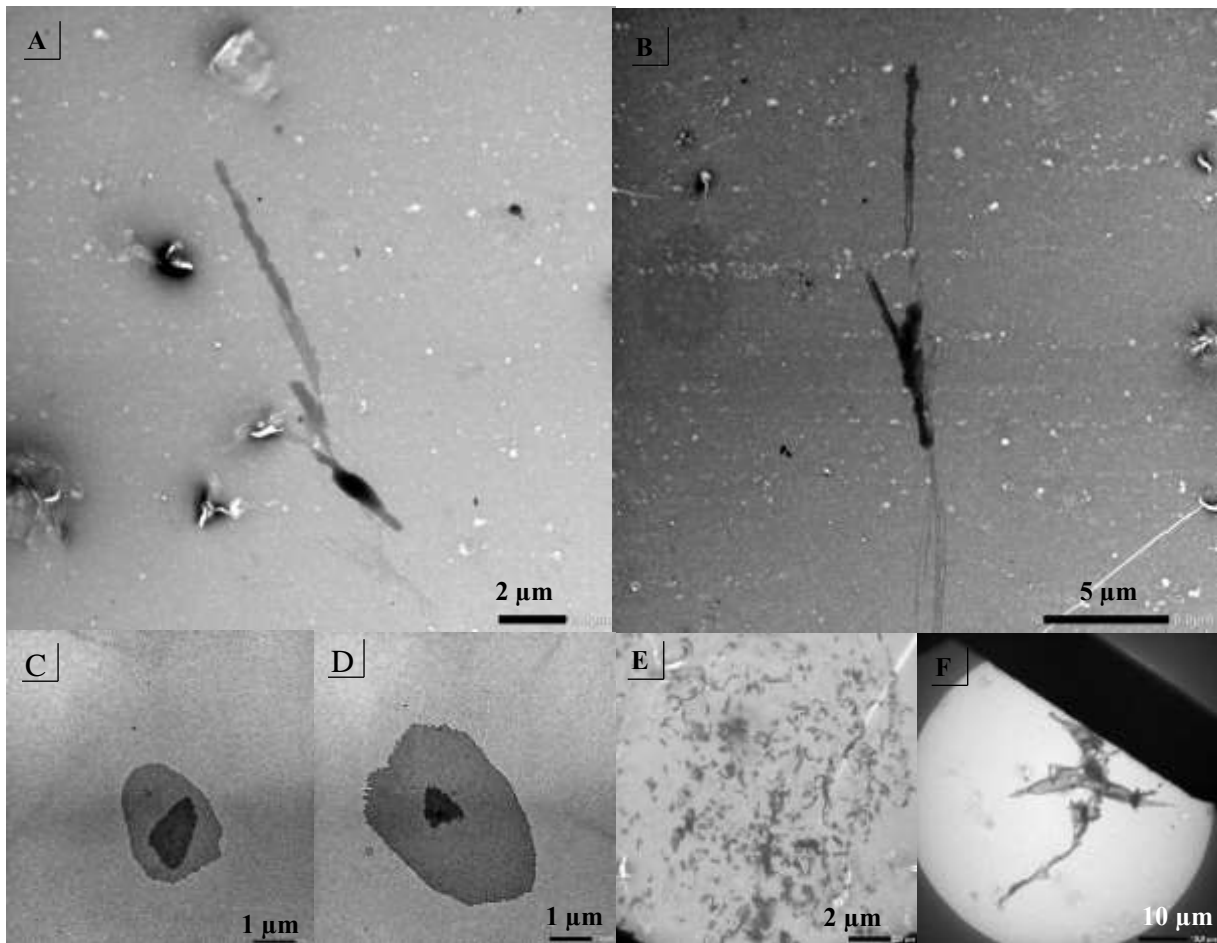
Figure 12. TEM images of self-assembled CP3 via nanoprecipitation in (A-B) DMF/H$_2$O at 1:4 using magnetic stirring, (C-D) DMF/H$_2$O at 1:4 using sonication bath (60 °C), (E-F) DMF/ethanol at 1:4 using magnetic stirring.

Comparing these results we could say that as in the case of CP1 a more efficient stirring method (sonication) and performing the self-assembly above the melting point of the PCL results in formation of better defined and more stable structures. This is explained by the higher substitution degree of CP1 compared to CP3, and the nature of the peptides. For CP1 the Tyr-Tyr peptide allows Pi-Pi stacking and H-bonding and a more hydrophobic character of the functional PCL block, leading to more defined structures. In contrast, with the hydrophilic RGD only H-bonding is expected in the considered conditions, with a lower hydrophobic character of the functional PCL block, leading to less defined structures.
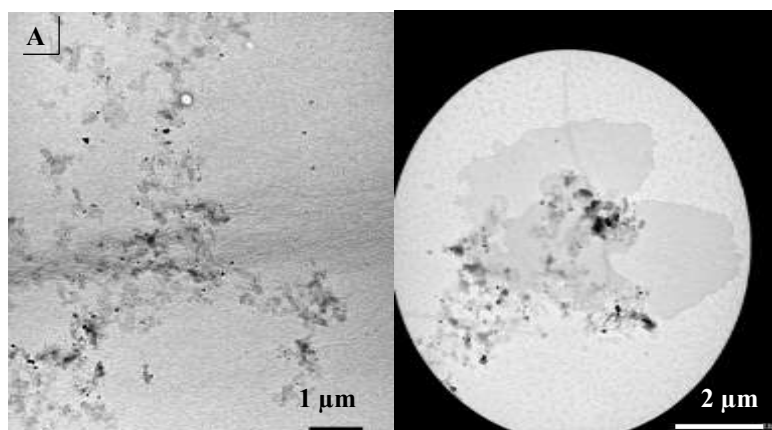
Figure 13. TEM images of self-assembled CP3 via nanoprecipitation in (A) DMSO/H$_2$O at 1:4 (B) DMSO/ethanol at 1:4 using magnetic stirring.

Table 1. Summary of optimised morphologies and self-assembly conditions for the three copolymers studied.

Copolymer	Micellization			Nanoprecipitation		
	Solvent	T (°C)	Morphology	Solvent	T (°C)	Morphology
C2	DMF/H$_2$O 1:4	60	flat aggregates	DMSO/H$_2$O 1:4	60	micelles
CP1	DMSO/H$_2$O 1:4	25	lamellar micelles	DMF/H$_2$O 1:4	60	flat lamellar micelles
CP3	DMF/H$_2$O 1:4	25	flat lamellar micelles	DMF/H$_2$O 1:4	60	flat lamellar micelles

Conclusions

The self-assembly of two amphiphilic PEG-*b*-PCL copolymers functionalized along the PCL block by peptides pending groups (with Tyr-Tyr or RGD units) was studied. Self-assembly was performed using two pathways; micellization and nanoprecipitation. Factors such as solvent / non-solvent system and ratio, concentration, temperature and stirring during self-assembly were studied and optimized. It was observed that using the ultrasonic bath at 60 °C, close to the melting temperature of the PCL block (60-65 °C), induced the formation of well-defined flat micelles and needles upon cooling. Such self-assembly is induced by the crystallization of the crystalline PCL blocks forming the core of the objects. Concentration does not play a very important role and the effect of working with more dilute stock solutions did not improve

results. On the other hand, the solvent used to solubilize the copolymer is important. DMSO seems to be a better solvent for the micellization of the two systems studied (better solvent for the PCL block) unlike the results of the nanoprecipitation where DMF results in better-defined structures. However, the impact of the non-solvent was important since with water defined micelles were formed as opposed to ethanol (at room temperature ethanol is a bad solvent for the PEG block and not a good solvent for the peptide). Based on the comparison with the PEG-*b*-PCL control, it could be stated that the presence of the peptide sequence is having a major effect on the self-assembly, since no defined structures were observed with PEG-*b*-PCL in opposition to the peptide-functional copolymers. The influence of the nature of the peptide was also very important for the self-assembly since among the 2 different peptide sequences tried the Tyr-Tyr directed the self-assembly toward the formation of more defined and stable structures due to its higher hydrophobicity and combination of Pi-Pi stacking and H-bonding.

Data availability

The raw/processed data required to reproduce these findings cannot be shared at this time as the data also forms part of an ongoing study.

References

[1] T.Z. Luo, K.L. Kiick, Collagen-Like Peptide Bioconjugates, Bioconjugate Chem. 28(3) (2017) 816-827.

[2] L.V. Arsenie, C. Pinese, A. Bethry, L. Valot, P. Verdie, B. Nottelet, G. Subra, V. Darcos, X. Garric, Star-poly(lactide)-peptide hybrid networks as bioactive materials, Eur. Pol. J. 139 (2020) 109990.

[3] H.G. Borner, Strategies exploiting functions and self-assembly properties of bioconjugates for polymer and materials sciences, Progress in Polymer Science 34(9) (2009) 811-851.

[4] H.R. Lakkireddy, D. Bazile, Building the design, translation and development principles of polymeric nanomedicines using the case of clinically advanced poly(lactide(glycolide))-poly(ethylene glycol) nanotechnology as a model: An industrial viewpoint, Adv. Drug Deliv. Rev. 107 (2016) 289-332.

[5] M. Alipour, M. Baneshi, S. Hosseinkhani, R. Mahmoudi, A.J. Arabzadeh, M. Akrami, J. Mehrzad, H. Bardania, Recent progress in biomedical applications of RGD-based ligand: From precise cancer theranostics to biomaterial engineering: A systematic review, J. Biomed. Mater. Res. A 108(4) (2020) 839-850.

[6] M. Nieberler, U. Reuning, F. Reichart, J. Notni, H.J. Wester, M. Schwaiger, M. Weinmuller, A. Rader, K. Steiger, H. Kessler, Exploring the Role of RGD-Recognizing Integrins in Cancer, Cancers 9(9) (2017) 116.

[7] Y. Fang, Y. Jiang, Y. Zou, F.H. Meng, J. Zhang, C. Deng, H.L. Sun, Z.Y. Zhong, Targeted glioma chemotherapy by cyclic RGD peptide-functionalized reversibly core-crosslinked multifunctional poly(ethylene glycol)-b-poly (epsilon-caprolactone) micelles, Acta Biomater. 50 (2017) 396-406.

[8] S.S. Wu, F.Y. Su, H.Y. Magee, D.R. Meldrum, Y.Q. Tian, cRGD functionalized 2,1,3-benzothiadiazole (BTD)-containing two-photon absorbing red-emitter-conjugated amphiphilic poly(ethylene glycol)-block-poly(epsilon-caprolactone) for targeted bioimaging, RSC Adv. 9(59) (2019) 34235-34243.

[9] D.H. Zhou, G. Zhang, Z.H. Gan, c(RGDfK) decorated micellar drug delivery system for intravesical instilled chemotherapy of superficial bladder cancer, J. Control.Release 169(3) (2013) 204-210.

[10] Y.B. Chi, S.S. Zhu, C. Wang, L.P. Zhou, L.M. Zhang, Z.Y. Li, Y.C. Dai, Glioma homing peptide-modified PEG-PCL nanoparticles for enhanced anti-glioma therapy, J. Drug Target. 24(3) (2016) 224-232.

[11] T. Kanazawa, H. Taki, H. Okada, Nose-to-brain drug delivery system with ligand/cell-penetrating peptidemodified polymeric nano-micelles for intracerebral gliomas, Eur. J. Pharm. Biopharm. 152 (2020) 85-94.

[12] P. Mandaviani, S. Bahadorikhalili, M. Navaei-Nigjeh, S.Y. Vafaei, M. Esfandyari-Manesh, A.H. Abdolghaffari, Z. Daman, F. Atyabi, M.H. Ghahremani, M. Amini, A. Lavasanifar, R. Dinarvand, Peptide functionalized poly ethylene glycol-poly caprolactone nanomicelles for specific cabazitaxel delivery to metastatic breast cancer cells, Mat. Sci. Eng. C-Mater. 80 (2017) 301-312.

[13] Y.Y. Guo, T. Gao, F. Fang, S. Sun, D.Y. Yang, Y.J. Li, S.W. Lv, A novel polymer micelle as a targeted drug delivery system for 10-hydroxycamptothecin with high drug-loading properties and anti-tumor efficacy, Biophys. Chem. 279 (2021) 106679.

[14] J.J. Li, S.Y. Xiao, Y.X. Xu, S. Zuo, Z.S. Zha, W.D. Ke, C.X. He, Z.S. Ge, Smart Asymmetric Vesicles with Triggered Availability of Inner Cell-Penetrating Shells for Specific Intracellular Drug Delivery, ACS Appl. Mater. Interfaces 9(21) (2017) 17727-17735.

[15] V. Pourcelle, J. Marchand-Brynaert, Light-Induced Functionalization of Amphiphilic Block Copolymers: Application to Nanoparticles for Drug Targeting, in: L.G. Rosa, F. Margarido (Eds.), Advanced Materials Forum V, Pt 1 and 22010, pp. 759-765.

[16] H.X. Wang, Q. Li, J. Yang, J.T. Guo, X.K. Ren, Y.K. Feng, W.C. Zhang, Comb-shaped polymer grafted with REDV peptide, PEG and PEI as targeting gene carrier for selective transfection of human endothelial cells, J. Mater. Chem. B. 5(7) (2017) 1408-1422.

[17] A. Al Samad, A. Bethry, O. Janouskova, J. Ciccione, C. Wenk, J.L. Coll, G. Subra, T. Etrych, F. El Omar, Y. Bakkour, J. Coudane, B. Nottelet, Iterative Photoinduced Chain Functionalization as a Generic Platform for Advanced Polymeric Drug Delivery Systems, Macromol. Rapid Commun. 39(3) (2018) 1700502.

[18] D. Grafahrend, J.L. Calvet, J. Salber, P.D. Dalton, M. Moeller, D. Klee, Biofunctionalized poly(ethylene glycol)-block-poly(epsilon-caprolactone) nanofibers for tissue engineering, J. Mater. Sci.: Mater. Med. 19(4) (2008) 1479-1484.

[19] J.S. Katz, S. Zhong, B.G. Ricart, D.J. Pochan, D.A. Hammer, J.A. Burdick, Modular Synthesis of Biodegradable Diblock Copolymers for Designing Functional Polymersomes, J. Am. Chem. Soc. 132(11) (2010) 3654.

[20] Z. Zhang, Y.X. Lai, L. Yu, J.D. Ding, Effects of immobilizing sites of RGD peptides in amphiphilic block copolymers on efficacy of cell adhesion, Biomaterials 31(31) (2010) 7873-7882.

[21] A. El Jundi, S. Buwalda, A. Bethry, S. Hunger, J. Coudane, Y. Bakkour, B. Nottelet, Double-Hydrophilic Block Copolymers Based on Functional Poly(epsilon-caprolactone)s for pH-Dependent Controlled Drug Delivery, Biomacromolecules 21(2) (2020) 397-407.

[22] A.T. Neffe, A. Zaupa, B.F. Pierce, D. Hofmann, A. Lendlein, Knowledge-Based Tailoring of Gelatin-Based Materials by Functionalization with Tyrosine-Derived Groups, Macromol. Rapid Commun. 31(17) (2010) 1534-1539.

[23] C. Bordes, V. Freville, E. Ruffin, P. Marote, J.Y. Gauvrit, S. Briancon, P. Lanteri, Determination of poly(epsilon-caprolactone) solubility parameters: Application to solvent substitution in a microencapsulation process, Int. J. Pharm. 383(1-2) (2010) 236-243.

[24] N.P. Iakimov, M.A. Zotkin, E.A. Dets, S.S. Abramchuk, A.M. Arutyunian, I.D. Grozdova, N.S. Melik-Nubarov, Evaluation of critical packing parameter in the series of polytyrosine-PEG amphiphilic copolymers, Colloid Polym. Sci. 299(10) (2021) 1543-1555.

[25] Z.Y. Li, R. Liu, B.Y. Mai, W.J. Wang, Q. Wu, G.D. Liang, H.Y. Gao, F.M. Zhu, Temperature-induced and crystallization-driven self-assembly of polyethylene-b-poly(ethylene oxide) in solution, Polymer 54(6) (2013) 1663-1670.

TOC

Peptide-guided self-assembly of polyethylene glycol-*b*-poly(ε-caprolactone-*g*-peptide) block copolymers

Ayman El Jundi[1‡], Matthias Mayor[2‡], Enrique Folgado[2], Chaimaa Gomri[2], Belkacem Tarek Benkhaled[2], Arnaud Chaix[2], Pascal Verdié[3], Benjamin Nottelet[1*], Mona Semsarilar[2*]

[1] Department of Polymers for Health and Biomaterials, IBMM (UMR5247), Univ Montpellier, CNRS, ENSCM, Montpellier, France

[2] Institut Européen des Membranes, IEM (UMR5635), Univ Montpellier, CNRS, ENSCM, Montpellier, France

[3] Synbio3, IBMM (UMR5247), Univ Montpellier, CNRS, ENSCM, Montpellier, France